

Effect Of Multiple Delamination on Composite Turbine Blade Subjected to Low Velocity Impact

Sudip Dey*

Mechanical Engineering Department,
Jadavpur University
Kolkata – 700032, INDIA

* E-mail of corresponding author: infosudip@gmail.com

Amit Karmakar

Mechanical Engineering Department,
Jadavpur University
Kolkata – 700032, INDIA
E-mail: shrikatha@yahoo.co.in

Abstract—This paper investigates on transient impact response of pretwisted composite conical shell panel which could be idealized as turbine blades. In the formulation, an eight noded quadratic isoparametric plate bending element is employed. A multipoint constraint algorithm is used to model the delamination crack. The modified Hertzian contact law is used to portray the impact parameters and Newmark's time integration scheme is utilized to solve the time dependent equations. Comparative analyses are carried out with respect to triggering impact parameters considering a spherical mass with low velocity impacted normally at the centre.

Keywords—low velocity impact; multiple delamination; conical shell; finite element

I. INTRODUCTION

A twisted conical shell panel with low aspect ratio could be portrayed as turbine blade. For light weight structures, composites are employed because of its high specific strength and stiffness. Even after having the broad pool of advantages of such composite structures, delamination causes the degradation of strength and can promote instability. The graphite-epoxy unidirectional cross-ply laminates because of its coupling properties are extensively employed for structural crashworthiness of advanced, weight efficient composite aircraft components. Composite shell structures are weak in strength through the thickness and are prone to high strain rate loading due to impact of foreign particles. The bird-hit or runway debris on the aircraft body is very common at the time of take-off or landing and level flight. The low velocity impact response of delaminated composites is the challenge to many advanced structural components like turbine blades. The energy waves promulgated during low velocity impact are much lower than the level of penetration and are sufficient to promote severe damage. Therefore, attention is required for understanding the transient impact behaviour of delaminated composite pretwisted conical shells centrally impacted by a spherical mass.

The pioneering investigation on impact response of composite plates was carried out by Sun and Chen [1] considering initial stress. Hu et al. [2] extended the investigation considering simply supported plates with delamination. Parhi et al. [3] studied the effect of bending and impact on composite plate using FEM. Yiming et al. [4] studied the dynamic response of elasto-plastic composite spherical shell under low velocity impact.

Khalili et al. [5] reported on low velocity impact modeling of composite shells and plates while Liu et al. [6] investigated on the time dependent responses of composite shells. The dynamic analyses of conical and hemispherical shells was investigated by Kowal-Michalska et al. [7] while similar study was also made by Gupta et al. [8] for composite cylindrical/conical shells. There is scanty and limited research work carried out in the field of delaminated composite pretwisted conical shells in the light of impact with low velocity. The present work investigates on the effects of delamination on transient impact response of composite pretwisted shallow conical shells. The finite element formulation is carried out based on Mindlin's theory assuming an isoparametric plate bending element with eight nodes. The modified Hertzian contact law [1] is employed to find out the contact force while Newmark's time integration scheme [9] is utilized to solve the time dependent equations.

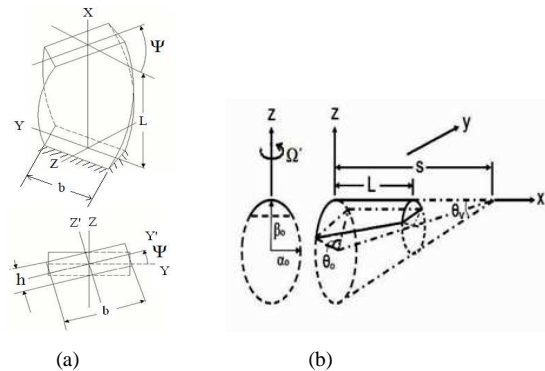


Fig. 1 (a) Plate under twist and (b) Conical shell geometry (Untwisted)

II. PRESENT MODEL AND GOVERNING EQUATION

The elliptical cross-section is assumed for a shallow conical shell with length L , uniform thickness h , width of reference b_0 , vertex angle θ_v and base subtended angle of cone θ_0 , as furnished in Fig. 1. $R_y(x,y)$ is the component of radius of curvature in the chordwise direction with $R_x = \infty$ and R_{xy} as the radius of twist. A shallow conical shell is expressed by its mid-surface as,

$$z = -\frac{1}{2} \left[\frac{x^2}{R_x} + 2 \frac{xy}{R_{xy}} + \frac{y^2}{R_y} \right] \quad (1)$$

The radius of twist (R_{xy}), twist angle (Ψ) and length (L) of shell are related as [10],

$$\tan \psi = -\frac{L}{R_{xy}} \quad (2)$$

The dynamic equilibrium equation is derived from Lagrange's equation of motion and global form equation is expressed as [11],

$$[M] \{\delta''\} + ([K] + [K_\sigma]) \{\delta\} = \{P(\Omega^2)\} + \{P\} \quad (3)$$

Here $[M]$ and $[K]$ are the mass and stiffness matrices, $\{P(\Omega^2)\}$ is nodal equivalent centrifugal forces and $\{\delta\}$ is global displacement vector. $[K_\sigma]$ depends on initial stress distribution and is obtained by iterative procedure [12],

$$([K] + [K_\sigma]) \{\delta\} = \{P(\Omega^2)\} \quad (4)$$

Under low velocity impact, force vector $\{P\}$ is expressed as

$$\{P\} = \{0 \ 0 \ 0 \dots P_C \dots 0 \ 0 \ 0\}^T \quad (5)$$

where P_C is the contact force and the equation of motion of rigid impactor is obtained as [1]

$$m_i \omega''_i + P_C = 0 \quad (6)$$

where m_i and ω''_i are mass and acceleration of impactor, respectively.

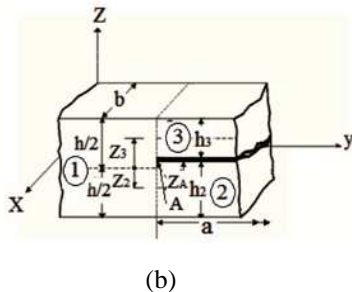
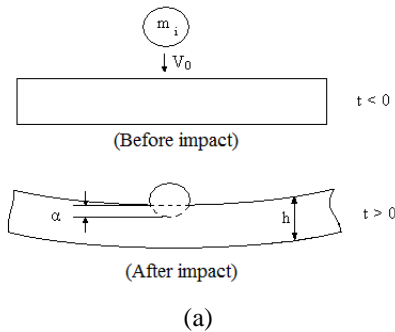


Fig. 2 (a) Before and after impact and (b) Element crack tip with delamination

A. Contact Force

The contact force depends on a contact law related with the indentation [Fig. 2(a)]. The contact law accounted for permanent indentation after unloading cycles. If k is the

contact stiffness and α_m is maximum local indentation, the contact force (P_C) during loading is evaluated as [1]

$$P_C = k \alpha^{1.5}, \quad 0 \leq \alpha \leq \alpha_m \quad (7)$$

where α is local indentation. The Hertzian contact theory is proposed as

$$k = \frac{4}{3} \sqrt{R} \frac{1}{\left[\frac{(1-\nu_i^2)}{E_i} + \frac{1}{E_{yy}} \right]} \quad (8)$$

where E_i and E_{yy} are the modulus of elasticity of the impactor and top layer of the laminate in transverse direction, respectively. Here, ν_i and R are the Poisson's ratio and radius of impact, respectively. Considering P_m as the maximum value of contact force and α_m as the maximum indentation, the contact forces (P_C) during the unloading and reloading are expressed as [1]

$$P_C = P_m \left[\frac{(\alpha - \alpha_o)}{(\alpha_m - \alpha_o)} \right]^{2.5} \text{ (for Undloading)} \quad (9)$$

$$P_C = P_m \left[\frac{(\alpha - \alpha_o)}{(\alpha_m - \alpha_o)} \right]^{1.5} \text{ (for Reloading)}$$

The permanent indentation (α_o) is expressed as [1]

$$\alpha_o = 0 \quad \text{when } \alpha_m < \alpha_{cr}, \text{ and} \quad (10)$$

$$\alpha_o = \beta_c (\alpha_m - \alpha_{cr}) \quad \text{when } \alpha_m \geq \alpha_{cr}$$

Here, $\beta_c = 0.094$ and $\alpha_{cr} = 1.667 \times 10^{-2}$ cm. The indentation (α) neglecting plate displacements along global x and y directions, is expressed as [13]

$$\alpha(t) = w_i(t) - w_p(x_c, y_c, t) \cos \psi \quad (11)$$

where w_i and w_p are the displacement of impactors and plate, respectively. The components of force at the impact point in global directions are given by [13]

$$P_{ix} = 0, \quad P_{iy} = P_C \sin \psi \quad \text{and} \quad P_{iz} = P_C \cos \psi \quad (12)$$

Now, Newmark's integration scheme [9] is employed to solve the equations of motion. The above equation (3) may be incorporated with each time step in the iteration form

$$[\bar{K}] \{\Delta\}_{t+\Delta t}^{i+1} = \frac{\Delta t^2}{4} \{P\}_{t+\Delta t}^i + [M] \{b\}_i \quad (13)$$

Here

$$[\bar{K}] = \frac{\Delta t^2}{4} [K] + [M] \quad (14)$$

$$\{b_i\} = \{\Delta\}_t + \Delta t \{\Delta'\}_t + 0.25 \Delta t^2 \{\Delta''\}_t \quad (15)$$

To solve the equation of motion of impactor, the above scheme is used. In Equation (15), i is the number of iterations within a time step. It is also to be noted that the modified contact force calculated from the previous iteration is taken as an input to solve the present

response $\{\Delta\}_{t+\Delta t}^{i+1}$. The iteration method will continue to meet the equilibrium criterion.

B. Multipoint Constraints

At the crack tip, nodal displacements of elements 2 and 3 as furnished in Fig. 2(b) are expressed as [14]

$$u_j = u'_j - (z - z'_j) \theta_{xj}, \quad v_j = v'_j - (z - z'_j) \theta_{yj}, \quad (16)$$

$$w_j = w'_j \quad (\text{where, } j = 2, 3)$$

The transverse displacements and rotations at a common node have values expressed as,

$$w_1 = w_2 = w_3 = w, \quad \theta_{x1} = \theta_{x2} = \theta_{x3} = \theta_x, \quad (17)$$

$$\theta_{y1} = \theta_{y2} = \theta_{y3} = \theta_y$$

In-plane displacements of all three elements at crack tip are equal and they are related as

$$u'_2 = u'_1 - z'_2 \theta_x, \quad v'_2 = v'_1 - z'_2 \theta_y, \quad (18)$$

$$u'_3 = u'_1 - z'_3 \theta_x, \quad v'_3 = v'_1 - z'_3 \theta_y$$

The strains at mid-plane between elements 2 and 3 are depicted as,

$$\{\varepsilon'\}_j = \{\varepsilon'\}_1 + z'_j \{k_1\} \quad (19)$$

where $\{\varepsilon'\}$ represents the strain vector and $\{k_1\}$ is the curvature vector. In-plane stress-resultants, $\{N\}$ and moment resultants, $\{M\}$ of elements 2 and 3 can be expressed as,

$$\{N\}_j = [A]_j \{\varepsilon'\}_1 + (z'_j [A]_j + [B]_j) \{k_1\} \quad (j=2, 3) \quad (20)$$

$$\{M\}_j = [B]_j \{\varepsilon'\}_1 + (z'_j [B]_j + [D]_j) \{k_1\} \quad (j=2, 3) \quad (21)$$

where $[A]$, $[B]$ and $[D]$ are the extension, bending-extension coupling and bending stiffness coefficients, respectively. At the delamination crack front, the equation of resultant forces $\{N\}$ and resultant moments $\{M\}$ are expressed as,

$$\{N\} = \{N\}_1 = \{N\}_2 + \{N\}_3 \quad (22)$$

$$\{M\} = \{M\}_1 = \{M\}_2 + \{M\}_3 + z'_2 \{N\}_2 + z'_3 \{N\}_3 \quad (23)$$

$$\{Q\} = \{Q\}_1 = \{Q\}_2 + \{Q\}_3 \quad (24)$$

The shape functions (S_i) are expressed as [9],

$$S_i = (1 + \zeta \zeta_i) (1 + \lambda \lambda_i) (\zeta \zeta_i + \lambda \lambda_i - 1) / 4 \quad (25)$$

(for $i = 1, 2, 3, 4$)

$$S_i = (1 - \zeta^2) (1 + \lambda \lambda_i) / 2 \quad (\text{for } i = 5, 7) \quad (26)$$

$$S_i = (1 - \lambda^2) (1 + \zeta \zeta_i) / 2 \quad (\text{for } i = 6, 8) \quad (27)$$

where ζ and λ are the local natural coordinates of the element.

III. DISCUSSION OF RESULTS

The computer codes are developed to address the transient impact behavior of conical shells under delamination. The results obtained from present computer codes are validated (Fig. 3 and Fig. 4) with the open literature [1,15]. Five degree of freedom at each node of isoparametric plate bending element (with 8 nodes) is considered in the present finite element formulation. Even by employing coarse mesh size (8 x 8 for full plate), excellent agreement is found in connection with validation of benchmark problem [1]. In the present analyses, determination of geometric stiffness arising out of centrifugal forces demands intensive programming as it is obtained by iterative procedure. This is essentially an initially stressed problem which is distinctly different from that of the benchmark problem wherein the structure is at statically prestressed condition. Thus the analyses could focus on both stationary and rotating structures. The following material properties are considered for the present analysis:

$$E_1 = 120 \text{ GPa}, \quad E_2 = 7.9 \text{ GPa}, \quad E_i = 210 \text{ GPa},$$

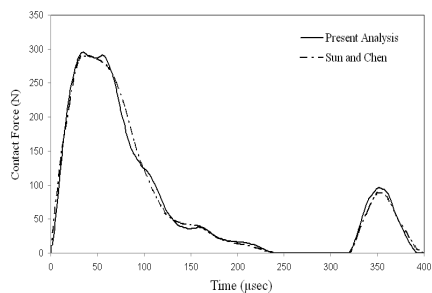
$$G_{12} = G_{23} = G_{13} = 5.5 \text{ GPa},$$

$$\rho = 1580 \text{ kg/m}^3, \quad \nu_i = \nu_{12} = 0.3$$

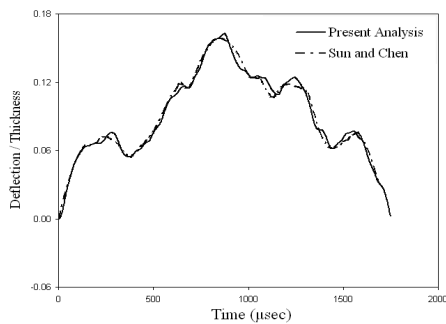
A. Low velocity impact response

In the present analysis, a sixteen layered graphite-epoxy composite cross-ply composite pretwisted conical shells is considered wherein numerical investigation is carried out with respect to mode of symmetry, number of delamination, twist angle and initial velocity of impactor (VOI). The arrangement of layers of laminate with delamination (where n = number of layers, nd = number of delamination) is shown in Fig. 5. The time histories of contact force at the central impact point are enumerated with the optimum time step of $\Delta t=1.0 \mu\text{-sec}$. The effect of twist and number of delamination on time histories of contact force for both symmetric and unsymmetric cross-ply composite conical shells is furnished in Fig. 6. For symmetric laminates, as the number layers increases, the coupling component becomes almost zero which in turn, leads to increase of elastic stiffness and as the elastic stiffness increases subsequently peak value of contact force also increases. It is observed that the contact force changes with the increase of twist and number of delamination for both symmetric and unsymmetric cross-ply laminate configurations. Because of the increment of stiffness, the peak value of contact force for symmetric laminate is found slightly higher than that of the same for unsymmetric one irrespective of number of delamination, twist angle. In general, due to increase of elastic stiffness as the number of delamination increases, it is found to reduce the peak value of contact force and subsequently observed to increase the contact duration. For unsymmetric laminate at $nd=8$, three consecutive peak values of contact force are observed irrespective of twist while the same is found absent for symmetric laminate. Hence, it can be inferred that number of delamination has significant effect on stiffness of cross-ply composite conical shells. The time histories of deflection/thickness

(Fig.7) show a linear trend during load-unloading cycle. After completion of loading-unloading cycle, the central deflection is observed to diverge with the change of other boundary conditions. After completion of loading-unloading cycle, the slope of deflection/thickness for symmetric laminate at $nd=8$ is found to be exorbitantly higher than that of the same at $nd=0, 1$ and 4 irrespective of twist angle while there is no such trend obtained for unsymmetric laminate. The variation of impactor's displacement with respect to time is furnished in Fig. 8.



(a)



(b)

Fig. 3 (a) Contact force and (b) Deflection/thickness with time for simply supported symmetric cross-ply composite plate (20 cm x 20 cm x 0.269 cm) centrally impacted by a spherical mass, with $n=10$, mass density of impactor= 7.96×10^{-5} N-sec²/cm⁴, time step (Δt)= 1.0μ -sec, $E_1=120$ GPa, $E_2=7.9$ GPa, $E_3=210$ GPa, $G_{12}=G_{23}=G_{13}=5.5$ GPa, $\rho=1580$ kg/m³, $\nu_1 = \nu_{12} = 0.3$, initial velocity of impactor (VOI)=3 m/s [1]

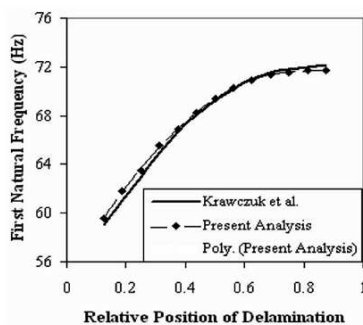


Fig. 4 Variation of fundamental natural frequency with relative position of the delamination for composite cantilever beam [15]

It is observed that after completion of loading-unloading cycle, the impactor's displacement curves are found to diverge due to variation in number of delamination depending on twist angle and laminate configuration. Higher number of delamination promotes

higher range and slope of impactor's displacement irrespective of laminate symmetry and twist angle.

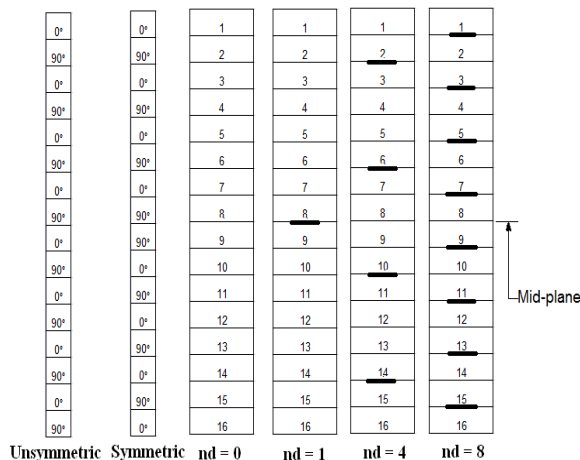
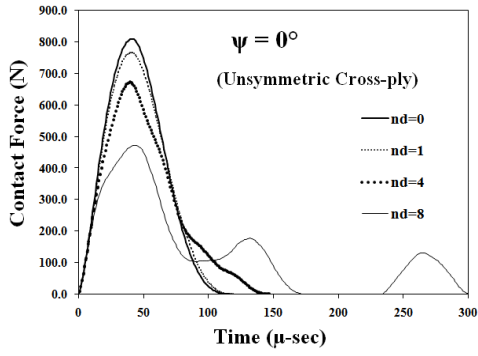


Fig. 5 Laminate configuration with location of delamination

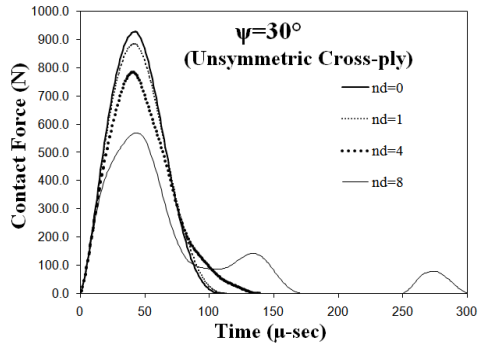
B. Effect of initial velocity of impactor

The initial velocity of impactor has significant effect on transient response of composite conical shells with multiple delamination as furnished in Fig. 9 and 10. In general, the peak value of contact force for untwisted cases is found to be lower than twisted cases. It is found that the peak value of contact force rises with higher initial velocity of impactor. This finding is the reestablishment of the results obtained by Sun and Chen [1]. In general, the deflection/thickness shows slight linear increment with respect to time during the loading-unloading cycle and immediately after it sharply increases.

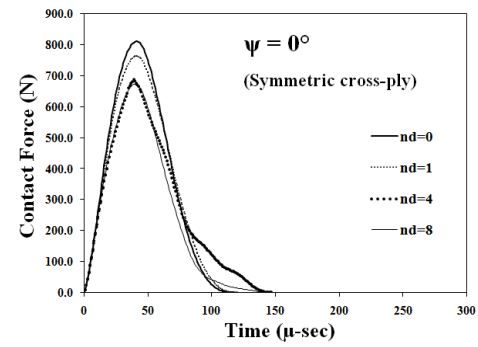
During loading-unloading cycle, it is also found that the slope of the curves of deflection/thickness versus time is directly proportional to initial velocities of impactor. For a specific initial velocity of impactor, the maximum value of contact force is identified for VOI=10 m/sec followed by VOI=5 m/sec, trailed by VOI=1 m/sec for both twisted and untwisted cross-ply composite conical shells. The slope of both deflection/thickness and impactor displacement for twisted as well as untwisted cases are identified to be maximum value for VOI=10 m/sec while the minimum value for VOI=1 m/sec. The striker's displacement is found directly proportional to striker's initial velocity within the computed time frame for both twisted and untwisted cases. The loading and unloading cycle time is observed to slightly reduce with the rise of initial velocity of impactor irrespective of twist angle.



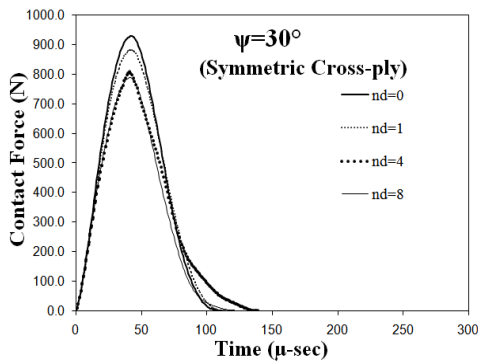
(a)



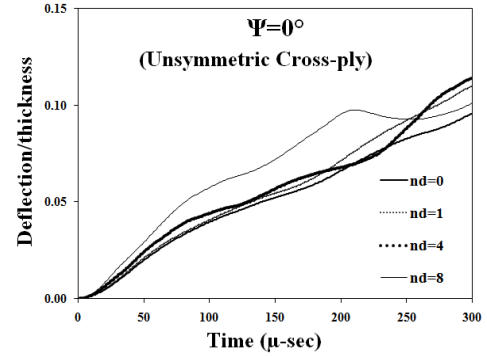
(b)



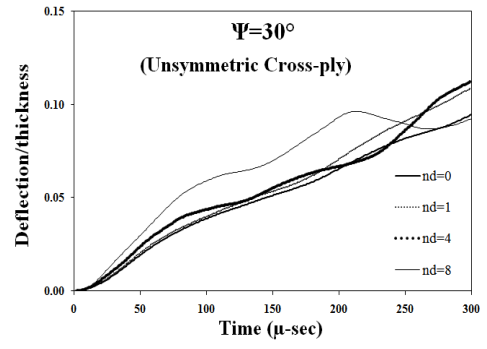
(c)



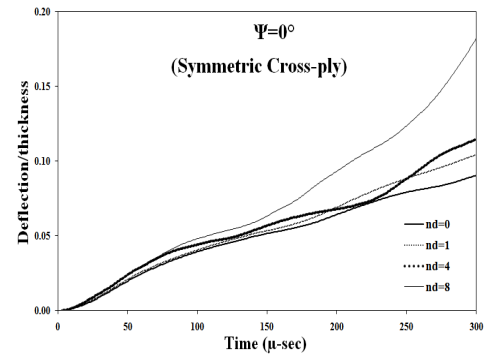
(d)



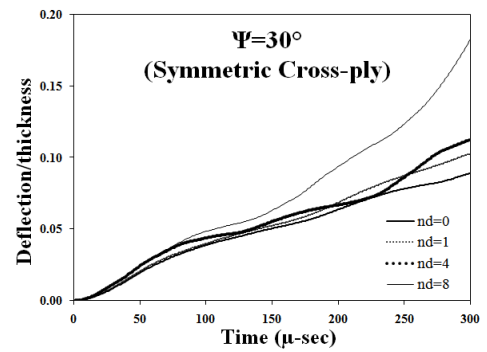
(a)



(b)



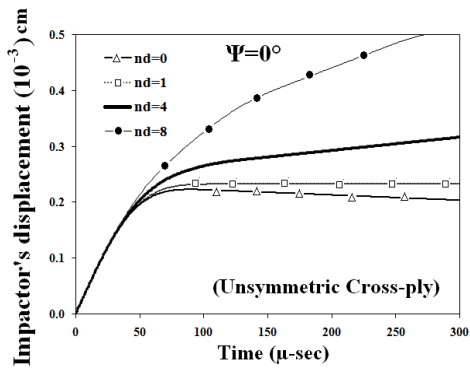
(c)



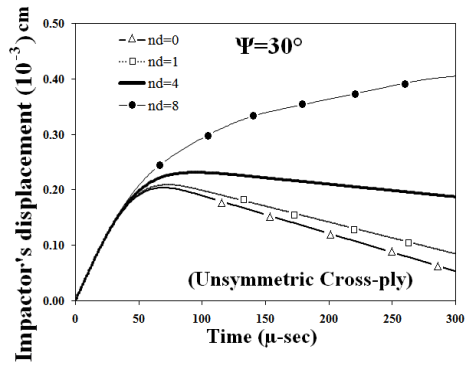
(d)

Fig. 6(a) to (d): Variation of contact force with time for symmetric and unsymmetric cross-ply composite conical shells considering $n=16$, $VOI=5$ m/s, $h=0.005$ m, $\theta_v=20^\circ$, $\theta_o=45^\circ$.

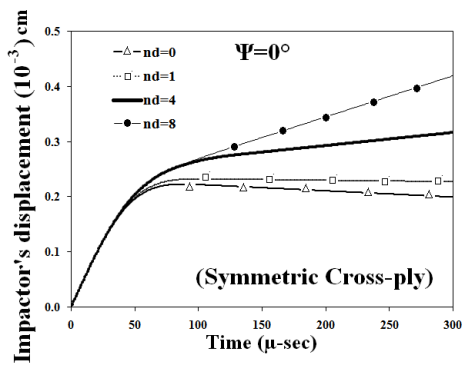
Fig. 7(a) to (d): Variation of deflection/thickness with time for symmetric and unsymmetric cross-ply composite conical shells considering $n=16$, $VOI=5$ m/s, $h=0.005$ m, $\theta_v=20^\circ$, $\theta_o=45^\circ$.



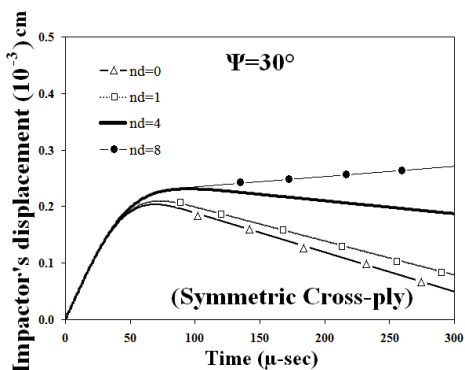
(a)



(b)

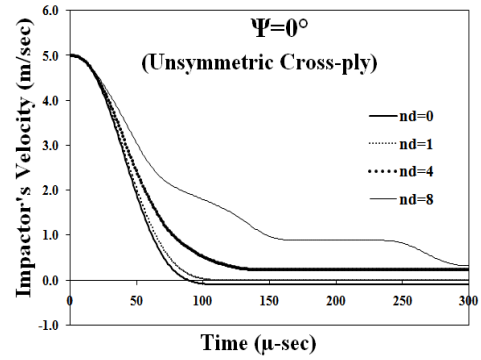


(c)

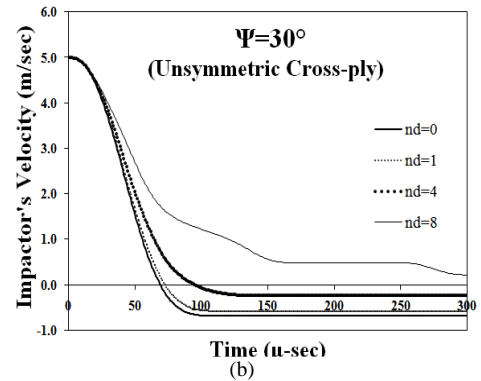


(d)

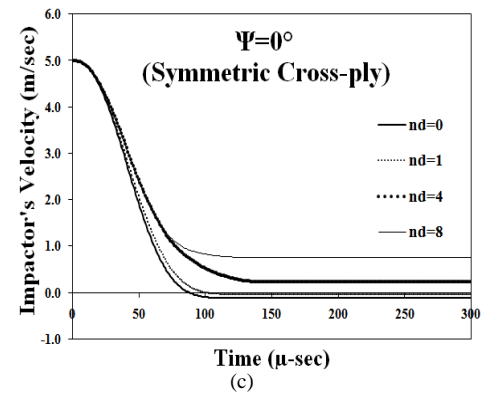
Fig. 8(a) to (d): Variation of impactor's displacement with time for symmetric and unsymmetric cross-ply composite conical shells considering $n=16$, $VOI=5$ m/s, $h=0.005$ m, $\theta_v=20^\circ$, $\theta_o=45^\circ$.



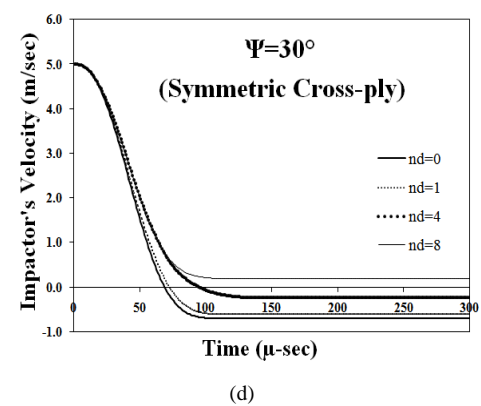
(a)



(b)

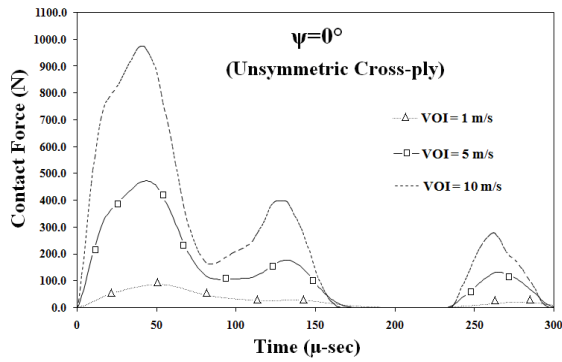


(c)

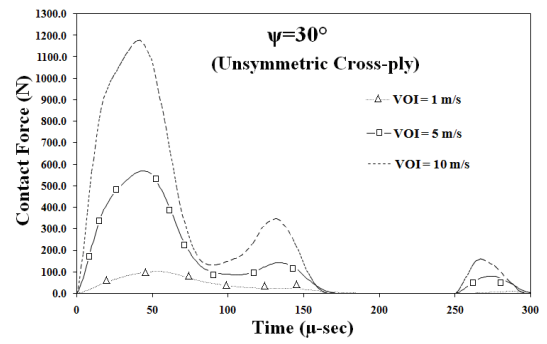


(d)

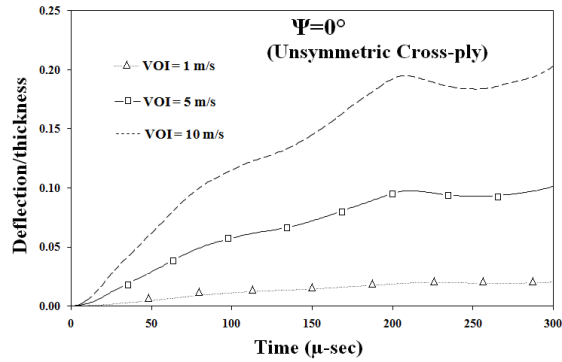
Fig. 9(a) to (d): Variation of impactor's velocity with time for symmetric and unsymmetric cross-ply composite conical shells considering $n=16$, $VOI=5$ m/s, $h=0.005$ m, $\theta_v=20^\circ$, $\theta_o=45^\circ$.



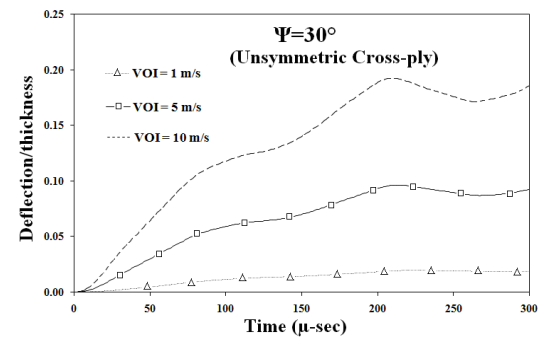
(a)



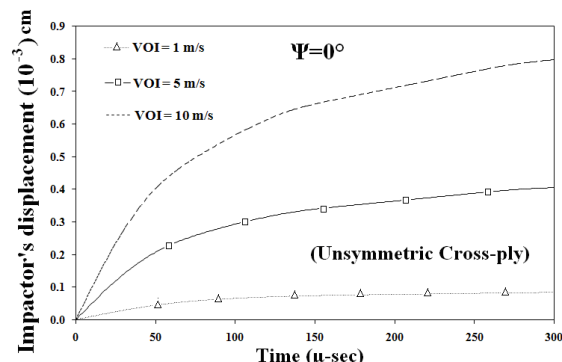
(e)



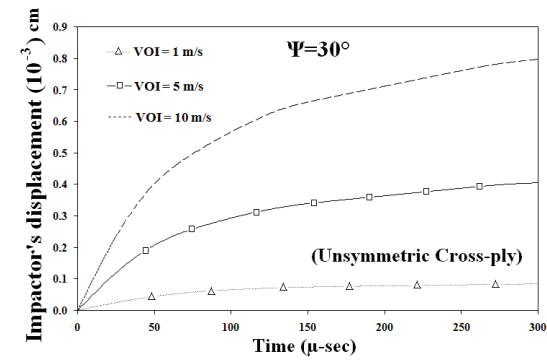
(b)



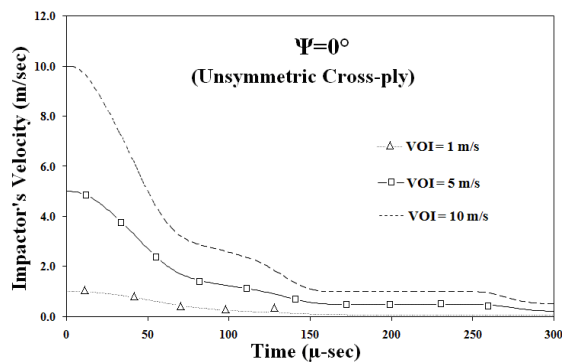
(f)



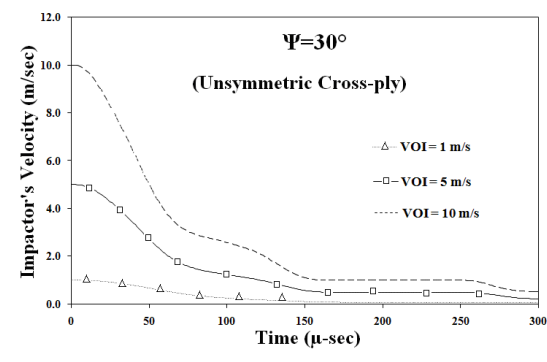
(c)



(g)



(d)



(h)

Fig. 10 (a) to (h): Effect of initial velocity of impactor on time histories of contact force, deflection/thickness, impactor's displacement and velocity for unsymmetric cross-ply composite conical shells considering $n=16$, $nd=4$, $VOI=5$ m/s, $h=0.005$ m, $\theta_v=20^\circ$, $\theta_c=45^\circ$.

IV. CONCLUSIONS

The computer codes based on the present formulation is validated with the results published in open literature and this can be employed to address the transient response for all cross-ply laminate configuration. The peak value of contact force is observed to increase with the increment of twist angle. The maximum value of contact force for untwisted cases is found to be lower than that of the same for the twisted one. The peak value of contact force is observed to decrease with the increase of number of delamination invariant to twist angle. It is observed that the peak value of contact force increases with higher initial velocity of the impactor. As the velocity of impactor increases, the maximum value of contact force is observed to increase irrespective of number of delamination and twist angle.

ACKNOWLEDGMENT

The first author acknowledges Dr. Sumanta Neogi and Dr. Arghya Nandi, Mechanical Engineering Department, Jadavpur University, Kolkata, India for their valuable suggestions and encouragement.

REFERENCES

- [1] C. T. Sun and J. K. Chen, "On the impact of initially stressed composite laminates", *Composite Materials*, Vol.19, pp.490-504, 1985.
- [2] N. Hu, H. Sekine, H. Fukunaga and Z. H. Yao, "Impact analysis of composite laminates with multiple delaminations", *Int. J. Impact Engineering*, vol. 22, pp.633-648, 1999.
- [3] P. K. Parhi, S. K. Bhattacharyya and P. K. Sinha, "Failure analysis of multiple delaminated due to bending and impact", *Bull. Mater. Sci.*, vol.24(2), pp.143-149, 2001.
- [4] Fu Yiming, Mao Yiqi and Tian Yanping, "Damage analysis and dynamic response of elasto-plastic laminated composite shallow spherical shell under low velocity impact", *Int. J. of Solids and Structures*, vol.47(1), pp.126-137, 2010.
- [5] S.M. R. Khalili, M. Soroush, A. Davar, O. Rahmani, "Finite element modeling of low-velocity impact on laminated composite plates and cylindrical shells", *Composite Structures*, vol.93(5), pp.1363-1375, 2011.
- [6] Chun-Chuan Liu, Feng-Ming Li, Wen-Hu Huang, "Transient wave propagation and early short time transient responses of laminated composite cylindrical shells", *Composite Structures*, vol.93(10), pp.2587-2597, 2011.
- [7] K. Kowal-Michalska, T. Kubiak, J. Swiniarski, "Influence of blast pressure modeling on the dynamic response of conical and hemispherical shells", *Thin-Walled Structures*, vol.49(5), pp.604-610, 2011.
- [8] A. K. Gupta, B. P. Patel and Y. Nath, "Continuum damage mechanics approach to composite laminated shallow cylindrical/conical panels under static loading", *Composite Structures*, vol.94(5), pp.1703-1713, 2012.
- [9] K. J. Bathe, "Finite Element Procedures in Engineering Analysis", New Delhi: PHI; 1990.
- [10] K. M. Liew, C. M. Lim and L. S. Ong, "Vibration of pretwisted cantilever shallow conical shells", *I. J. Solids Structures*, vol.31(18), pp.2463-74, 1994.
- [11] A. Karmakar and P. K. Sinha, "Failure analysis of laminated composite pretwisted rotating plates", *Journal of Reinforced Plastics and Composites*, vol.20(14-15), pp.1326-1357, 2001.
- [12] S. Sreenivasamurthy and V. Ramamurti, "Coriolis effect on the vibration of flat rotating low aspect ratio cantilever plates", *J. Strain Analysis*, vol.16(2), pp.97-106, 1981.
- [13] A. Karmakar and P. K. Sinha, "Finite element transient dynamic analysis of laminated composite pretwisted rotating plates subjected to impact", *Int. J. of Crashworthiness*, vol.3(4), pp.379-391, 1998.
- [14] C. K. Gim, "Plate finite element modelling of laminated plates", *Composite Structures*, vol.52, pp.157-168, 1994.
- [15] M. Krawczuk, W. Ostachowicz and A. Zak, "Dynamics of cracked composite material structures", *Computational Mechanics*, vol.20, pp.79-83, 1997.